Fingering of Chemical Fronts in Porous Media

A. De Wit

Service de Chimie Physique and Center for Nonlinear Phenomena and Complex Systems, Université Libre de Bruxelles, CP 231, Campus Plaine, 1050 Brussels, Belgium

(Received 22 January 2001; published 11 July 2001)

The influence of chemical reactions on the hydrodynamical fingering instability is analyzed for miscible systems in porous media. Using a realistic reaction scheme, it is shown that the stability of chemical fronts towards density fingering crucially depends on the width and the speed of the front which are functions of chemical parameters. The major difference between the pure and chemically driven fingering is that, in the presence of chemical reactions, the dispersion curves do not vary in time which has important practical experimental consequences. Good agreement with recent experimental data is found.

DOI: 10.1103/PhysRevLett.87.054502 PACS numbers: 47.20.Bp, 47.55.Mh, 47.70.Fw, 82.40.Ck

Fingering of an interface is a common phenomenon encountered in fields as diverse as petroleum recovery [1], combustion [2], electrochemical deposition [3], reaction-diffusion systems [4–6], etc. Because of the influence of such fingers on the physical and chemical processes, numerous studies have analyzed to what extent the fingering instability can be affected, for instance, by heterogeneities of the medium [7], the non-Newtonian character of flows [8], particle accretion [9], the presence of a magnetic field [10], etc.

In this Letter, we show that chemical reactions profoundly affect the fingering of an interface. To do so, the stability of a chemical front towards buoyancy effects is studied for miscible systems in a porous medium or Hele-Shaw cell. The chemical reaction can diminish the local density causing ascending fronts to be buoyantly unstable giving rise to complex fingering phenomena. The buoyancy-driven instability of reaction-diffusion fronts has already been studied in laterally extended systems both experimentally [11,12] and theoretically [13–18]. Attempts to compare such theories with recent experiments do not, however, provide good agreement [12]. We show here that the stability towards fingering of such interfaces undergoing chemical reactions depends crucially on the width and the speed of the front which are functions of the chemical parameters. This changes dramatically our understanding of the coupling between chemistry and hydrodynamical instabilities and suggests a new interpretation of experiments.

Our system is an infinite two-dimensional porous medium with the gravity field $\underline{g}$ oriented along x (Fig. 1). In this system, a solution of concentration c_1 and density ρ_1 is the steady state of the reaction-diffusion system which invades a different steady state above it with speed v. In the upper region, the concentration is taken without loss of generality to be equal to zero and the density is $\rho_0 > \rho_1$. The system can be described by Darcy's equations (1)–(2) for the velocity field $\underline{u}$ coupled to an advection-reaction-diffusion equation (3) for c [4,19]:

$$\underline{\nabla} \cdot \underline{u} = 0, \tag{1}$$

$$\underline{\nabla} p = -\frac{\mu}{\kappa}\,\underline{u} + \rho(c)\underline{g}, \tag{2}$$

$$\frac{\partial c}{\partial t} + \underline{u} \cdot \underline{\nabla} c = D\nabla^2 c - \gamma c(c - c_1)(c + c_2). \tag{3}$$

Here the viscosity μ, permeability κ, and diffusion coefficient D are constant while p represents the pressure. The density ρ is assumed to depend linearly on the local concentration c of the solute as $\rho(c) = \rho_1 + (\rho_o - \rho_1)(1 - c/c_1)$. In writing (2), we make use of Boussinesq's approximation assuming that changes in density can be neglected everywhere except in the buoyancy term $\rho\underline{g}$ in Darcy's law [19]. The reaction term is chosen as a simple kinetic expression allowing chemical fronts between two steady states [20–22]. The kinetic constant γ and the concentrations c_1 and c_2 of the model can be explicit in terms of experimental parameters as is shown later for a specific example. The hydrostatic pressure $\rho_1\underline{g}$ can be incorporated in the pressure term if we define $\underline{\nabla} p^* = \underline{\nabla} p - \rho_1\underline{g}$. To nondimensionalize the equations, we define a characteristic speed $U = \Delta\rho g\kappa/\nu$, where $\Delta\rho = (\rho_0 - \rho_1)/\rho_0$

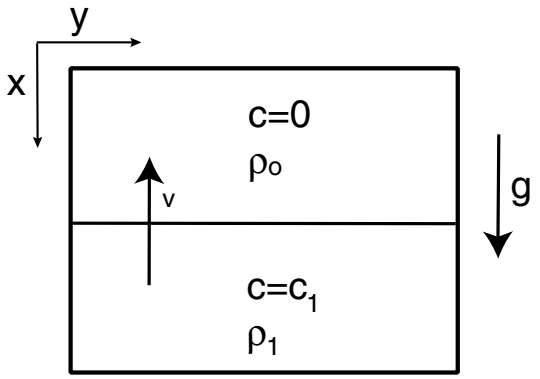

FIG. 1. Sketch of the system.

 0031-9007/01/87(5)/054502(4)$15.00

and $\nu = \mu/\rho_0$ is the kinematic viscosity. As characteristic length and time scales, we use, respectively, $L = D/U$ and $\tau = D/U^2$. We then introduce the nondimensional variables $x' = x/L, y' = y/L, \underline{u}' = \underline{u}/U, t' = t/\tau, p' = p^*\kappa/\mu D, \rho' = \rho/\rho_0, c' = c/c_1$ where now $0 \leq c' \leq 1$. As the chemical front is moving upwards with velocity v in the direction of negative x, we next switch to the moving frame $z = x' + vt'$. Dropping all the primes, the dimensionless evolution equations become

$$\underline{\nabla} \cdot \underline{u} = 0, \tag{4}$$

$$\underline{\nabla} p = -\underline{u} + (1 - c)\underline{e}_x, \tag{5}$$

$$\frac{\partial c}{\partial t} + v\frac{\partial c}{\partial z} + \underline{u} \cdot \underline{\nabla} c = \nabla^2 c - \alpha c(c - 1)(c + d), \tag{6}$$

where $d = c_2/c_1$. The dimensionless kinetic constant $\alpha = D\gamma c_1^2/U^2$ is the ratio between the dispersive time scale and the chemical time scale, i.e., the Damköhler number. The system of equations (4)–(6) admits as a base state

$$c_0 = c_0(z, t), \tag{7}$$

$$\underline{u}_0 = 0, \qquad p_0 = p_0(z, t), \tag{8}$$

where $p_0(z, t)$ is the base profile of pressure, solution of Eq. (5) for the given concentration profile $c_0(z, t)$. Linearizing equations (4)–(6) around the base state (7) and (8) and expanding the perturbations in Fourier modes as $(u_1, w_1, p_1, c_1) = (\delta u, \delta w, \delta p, \delta c)(z, t_0)e^{iky}e^{\sigma t}$, we get, after eliminating w_1 and p_1,

$$\left[\frac{d^2}{dz^2} - k^2\right]\delta u = k^2 \delta c, \tag{9}$$

$$\left[\frac{d^2}{dz^2} - v\frac{d}{dz} - \alpha[3c_0^2 + 2c_0(d - 1) - d] - \sigma - k^2\right]\delta c = \frac{dc_0}{dz}\delta u, \tag{10}$$

where σ is the growth rate of the perturbations and k is their wave number while the subscript zero means computed for $c = c_0(z, t)$. The perturbations δu and δc tend to zero as $z \to \pm\infty$. Equations (9) and (10) are two coupled ordinary differential equations defining an eigenvalue problem for σ whose solution will give the dispersion relation $\sigma = \sigma(k)$. In most cases, the eigenvalue problem cannot be solved analytically and we therefore resort to numerical simulations. To do so, we perform initial value integration of Eqs. (9) and (10) expressed in the stream function formalism [19] using a pseudospectral numerical scheme [4,23]. Matching the growth in time of each Fourier mode of c by an exponential gives the growth rate σ for each wave number k. The problem is independent of any Rayleigh number and depends only on the two chemical parameters α and d controlling the width and the velocity v of the wave. This result is in sharp contrast with some previous theoretical work [15,16,18] which assume a flat front and express all results in terms of a Rayleigh number $Ra = Ua/D$ constructed with the gap width a of a Hele-Shaw cell. These works do not explain the influence of chemical parameters on the stability of the front [12] which is non-negligible as we show next in a parametric study.

Let us first analyze the $\alpha = 0$ limiting case of pure density fingering without chemical reactions. The base concentration profile is then given by

$$c_0(z, t) = \frac{1}{2}\left[1 + \mathrm{erf}\left(\frac{z}{2\sqrt{t}}\right)\right]. \tag{11}$$

The width of the front increases diffusively in time due to the mixing of the two miscible solutions. At time $t = 0$, the concentration profile (11) takes the form of a step function. Following the reasoning of Tan and Homsy [24,25], we find analytically in this limit

$$\sigma = \frac{k}{2}[1 - k - \sqrt{k^2 + 2k}], \quad \text{for } \alpha = 0, t = 0. \tag{12}$$

This dispersion relation is that for viscous fingering [24] in the special case where the mobility ratio $R = \ln(\mu_2/\mu_1) = 1$ stressing the similarity between viscous and density fingering [26]. The band of unstable modes admits a cutoff wave number $k_c = 1/4$ and a most unstable mode with $k_m = 0.118$ and $\sigma_m = 0.0225$. This is coherent with numerical results by Vasquez *et al.* [18]. At later times, the base state profile $c_0(z, t)$ evolves according to expression (11) and the dispersion curve is obtained numerically. Figure 2 shows that the dispersion curves for $\alpha = 0$ feature a range of unstable modes and a maximum growth rate that decrease in the course of time because of a diffusive stabilization of the system when the two solutions start to mix.

For $\alpha \neq 0$, the reaction-diffusion system (6) with $\underline{u} = 0$ admits several front solutions depending on the

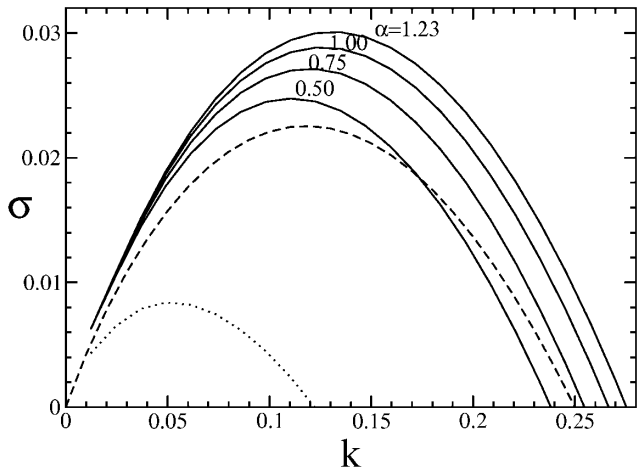

FIG. 2. Dispersion curves in dimensionless variables obtained for $d = 0.0021$ and variable α, i.e., varying both the width and the velocity of the chemical front. The dashed and dotted curves are the dispersion curves for pure density fingering ($\alpha = 0$) at times $t = 0$ and $t = 150$, respectively.

parameters [27]. We analyze here the "pushed" front solution for which an analytical expression exists [21]:

$$c_0(z) = \frac{1}{1 + e^{-\sqrt{\alpha/2}\,z}}, \qquad (13)$$

where the chemical front speed $v = \sqrt{\alpha/2}(1 + 2d)$. The width of the front is constant in time and is inversely proportional to α; hence the higher α, the steeper and the more rapid the chemical front. The $\alpha \to \infty$ limit of a step function front is not well defined in Eq. (10) as the step function is not a physical solution of the reaction-diffusion equation. We therefore resort to numerical calculations to find the dispersion curves comparing the situation with and without chemical reactions in Fig. 2. An important difference between the pure and chemically driven fingering is that chemical reactions maintain the width of the front *constant in time* and hence the dispersion curves for $\alpha \neq 0$ *do not vary in time*. This means that dispersion curves are likely to be measured experimentally with more accuracy for fingering of asymptotic chemical fronts than for pure density fingering for which initial condition and time of measurement are important. Initial conditions may remain important, however, if the chemical front is established only after a transient. For the value of d chosen here, the curves for the chemical fingers are systematically above the initial time limiting case (12) for pure fingering. Reactive fingers are thus here more unstable than their nonreactive equivalent for the same density ratio. Note that, at fixed d, an increase in the dimensionless kinetic constant α (and hence of the velocity v) leads to a more unstable situation (Fig. 2). This means that sharper waves traveling with a larger velocity will develop fingers with a larger growth rate. This can be understood as an increase of α sharpens the chemical front counterbalancing the stabilization by diffusion. Increasing α also leads to smaller wavelengths which is likely to favor tip splittings in the nonlinear regime.

Let us now keep α constant while increasing d. As can be seen in Fig. 3, this leads to a stabilization of the waves. This can be understood as such a variation of parameters results in an increase of the velocity of the wave while keeping its width constant, i.e., decreasing the overall destabilizing force. Note furthermore that, for the set of parameters of Fig. 3, the growth rate of the chemical fingers is smaller than the initial growth rate of pure density fingering, indicating that the relative stability of the pure and chemical fingers is strongly dependent on the (α, d) couple of parameters.

We now compare quantitatively our predictions with experimental dispersion curves obtained recently by Böckmann and Müller on the buoyancy fingering of iodate-arsenious acid (IAA) reaction-diffusion fronts in a Hele-Shaw setup [12]. The IAA reaction can quantitatively be modeled by Eqs. (1)–(3) and (13) with $c = [I^-]$, $c_1 = [IO_3^-]_0$, $c_2 = k_a/k_b$, $\gamma = k_b[H^+]^2$, where k_a and k_b are kinetic constants [20,22].

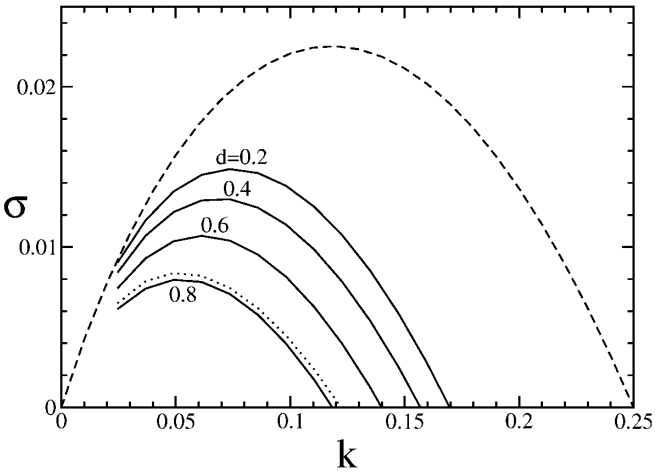

FIG. 3. Dispersion curves in dimensionless variables keeping $\alpha = 0.1$ and varying d, i.e., keeping the width of the wave constant and increasing its velocity. The dashed and dotted curves are as in Fig. 2.

As experimental data [28], we use $\Delta\rho = 1.30 \times 10^{-4}$ and a gap width $a = 0.46$ mm with the permeability $\kappa = a^2/12$ for which we get $d = 0.0021$ and $\alpha = 1.71$. While previous theoretical dispersion curves obtained by neglecting the effect of the width of the front [15,16] are off by more than 50% [12], our dispersion curve is in good agreement with experimental data (see Fig. 4). The comparison should be made for the band of modes with positive growth rates as the experimental data points with negative growth rates have an experimental low reliability as explained in [12]. Note that the experimental data are given

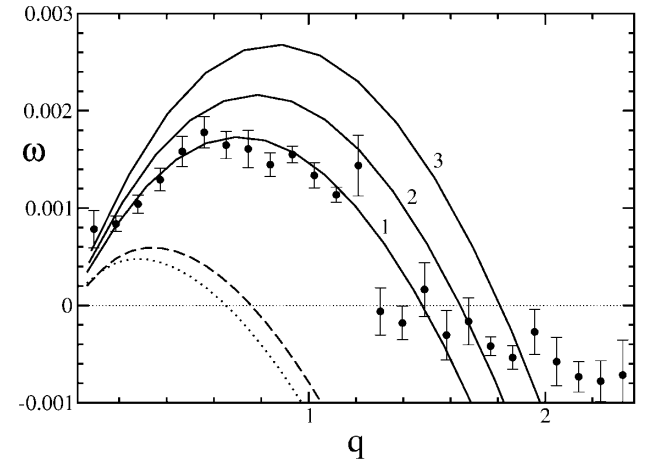

FIG. 4. Dispersion curves in the dimensionless growth rate $\omega = Ra^2\sigma/S_c$ and wave number $q = Ra\,k$ used in Ref. [12], where $S_c = \nu/D$ is the dimensionless Schmidt number. Experimental data are shown as dark circles. The dashed and dotted curves are the pure density fingering dispersion relations ($\alpha = 0$) corresponding to dimensional times of 200 and 480 s, respectively, which delimit roughly the time interval used in experiments for growth rate determination [29]. The solid curves are the dispersion curves when chemical reactions are taken into account using $\Delta\rho = 1.30 \times 10^{-4}$ and $a = 0.46$ mm (1); $a = 0.48$ mm (2); $a = 0.50$ mm (3).

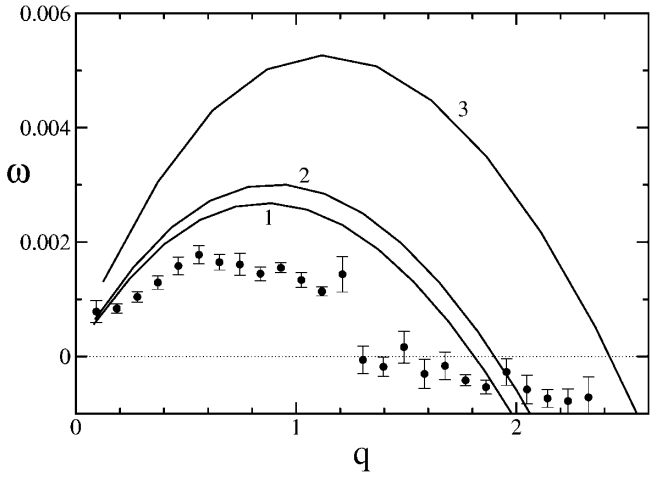

FIG. 5. Effect of the density difference on the dispersion curve. The dimensionless variables are the same as in Fig. 4. $\Delta\rho = 1.30 \times 10^{-4}$ (1); 1.40×10^{-4} (2); 2.00×10^{-4} (3) for $a = 0.50$ mm.

for $a = (0.50 \pm 0.05)$ mm [29]. Figure 4 shows that the theoretical dispersion curve is very sensitive to the value of the gap width [12] as the dimensionless parameter α scales like a^{-4} for a Hele-Shaw cell. The best fit is obtained with $a = 0.46$ mm which is in the experimental range of a. Uncertainty also exists regarding the values of $\Delta\rho$ (and hence of α) which lie in the range from 1.30×10^{-4} to 2.00×10^{-4} [12,29,30]. Figure 5 indicates that theoretical curves are in better agreement with experimental data for the lowest bound of this range of density ratios.

Let us recall that for the IAA reaction, $\alpha \sim [H^+]^2[IO_3^-]_0^2$ while $d \sim [IO_3^-]_0^{-1}$. Based on our previous parametric study in dimensionless variables of Figs. 2 and 3, we understand that an increase of pH in the IAA reaction keeping all other parameters constant (i.e., increasing α while keeping d constant) should give sharper waves traveling with a larger velocity and developing fingers with a larger growth rate and smaller wavelengths [14]. Diminishing $[IO_3^-]_0$ keeping the product $[H^+]^2[IO_3^-]_0^2$ constant (i.e., increasing d for a fixed α) should on the contrary lead to a stabilization of the waves.

In conclusion, we have shown that chemical reactions quantitatively affect the stability criteria of the density fingering instability. Good agreement with experimental dispersion curves is obtained. Experimental conditions to test the effect of pH and other concentration changes on the stability towards fingering of iodate-arsenious acid reaction fronts are proposed.

This work has benefited from numerous enlightening discussions with G. M. Homsy who is gratefully acknowledged. I also thank M. Böckmann, S. C. Müller, G. Dewel, P. Borckmans, K. Showalter, and H. Sevcikova for fruitful discussions. This work is financially supported by the FNRS (Belgium), ESA, and the Belgian FRFC program.

[1] G. M. Homsy, Annu. Rev. Fluid Mech. **19**, 271 (1987).
[2] O. Zik *et al.,* Phys. Rev. Lett. **81**, 3868 (1998).
[3] J. R. de Bruyn, Phys. Rev. Lett. **74**, 4843 (1995); J. Elezgaray *et al.,* Phys. Rev. Lett. **84**, 3129 (2000).
[4] A. De Wit and G. M. Homsy, J. Chem. Phys. **110**, 8663 (1999), and references therein.
[5] K. Eckert and A. Grahn, Phys. Rev. Lett. **82**, 4436 (1999); Y. Nagatsu and T. Ueda, AIChE J. (to be published).
[6] I. R. Epstein and J. A. Pojman, *An Introduction to Nonlinear Chemical Dynamics* (Oxford University Press, Oxford, 1998).
[7] C. T. Tan and G. M. Homsy, Phys. Fluids A **4**, 1099 (1992); H. A. Tchelepi *et al.,* Phys. Fluids A **5**, 1558 (1993); C. Y. Chen and E. Meiburg, J. Fluid Mech. **371**, 233 (1998); A. De Wit and G. M. Homsy, J. Chem. Phys. **107**, 9609 (1997); E. Camhi *et al.,* J. Fluid Mech. **420**, 259 (2000), and references therein.
[8] K. Makino *et al.,* Phys. Fluids **7**, 455 (1995); E. C. Poiré and M. Ben Amar, Phys. Rev. Lett. **81**, 2048 (1998); L. Kondic *et al.,* Phys. Rev. Lett. **80**, 1433 (1998); A. Lindner *et al.,* Phys. Rev. Lett. **85**, 314 (2000).
[9] H. Tang *et al.,* Phys. Rev. Lett. **85**, 2112 (2000).
[10] C. Flament *et al.,* Phys. Fluids **10**, 2464 (1998); G. Pacitto *et al.,* Phys. Rev. E **62**, 7941 (2000); M. Widom and J. A. Miranda, J. Stat. Phys. **93**, 411 (1998).
[11] M. R. Carey *et al.,* Phys. Rev. E **53**, 6012 (1996).
[12] M. Böckmann and S. C. Müller, Phys. Rev. Lett. **85**, 2506 (2000).
[13] B. F. Edwards *et al.,* Phys. Rev. A **43**, 749 (1991).
[14] D. A. Vasquez *et al.,* J. Chem. Phys. **98**, 2138 (1993).
[15] J. Huang *et al.,* Phys. Rev. E **48**, 4378 (1993).
[16] J. Huang and B. F. Edwards, Phys. Rev. E **54**, 2620 (1996).
[17] J. Zhu, Phys. Fluids **10**, 775 (1998).
[18] D. A. Vasquez *et al.,* J. Chem. Phys. **104**, 9926 (1996).
[19] E. Holzbecher, *Modeling Density-Driven Flow in Porous Media* (Springer-Verlag, Berlin, 1998).
[20] A. Hanna, A. Saul, and K. Showalter, J. Am. Chem. Soc. **104**, 3838 (1982).
[21] A. Saul and K. Showalter, in *Oscillations and Traveling Waves in Chemical Systems,* edited by R. J. Field and M. Burger (Wiley, New York, 1985).
[22] J. H. Merkin and H. Sevcikova, Phys. Chem. Chem. Phys. **1**, 91 (1999).
[23] C. T. Tan and G. M. Homsy, Phys. Fluids **31**, 1330 (1988).
[24] C. T. Tan and G. M. Homsy, Phys. Fluids **29**, 3549 (1986).
[25] A. Rogerson and E. Meiburg, Phys. Fluids A **5**, 1344 (1993).
[26] O. Manickam and G. M. Homsy, J. Fluid Mech. **288**, 75 (1995).
[27] W. van Saarloos and P. C. Hohenberg, Physica (Amsterdam) **56D**, 303 (1992).
[28] As typical experimental values, we use $k_a = 4.5 \times 10^3\ M^{-3}\,s^{-1}$, $k_b = 4.5 \times 10^8\ M^{-4}\,s^{-1}$, $[H^+] = 6.45 \times 10^{-3}$ M, $[IO_3^-]_0 = 4.8 \times 10^{-3}$ M, $D = 2.04 \times 10^{-5}\ cm^2/s$, $g = 980.665\ cm/s^2$, $\rho_0 = 1.002\ g/cm^3$, and $\nu = 0.0099\ cm^2/s$.
[29] M. Böckmann (private communication).
[30] J. A. Pojman *et al.,* J. Phys. Chem. **95**, 1299 (1991).